

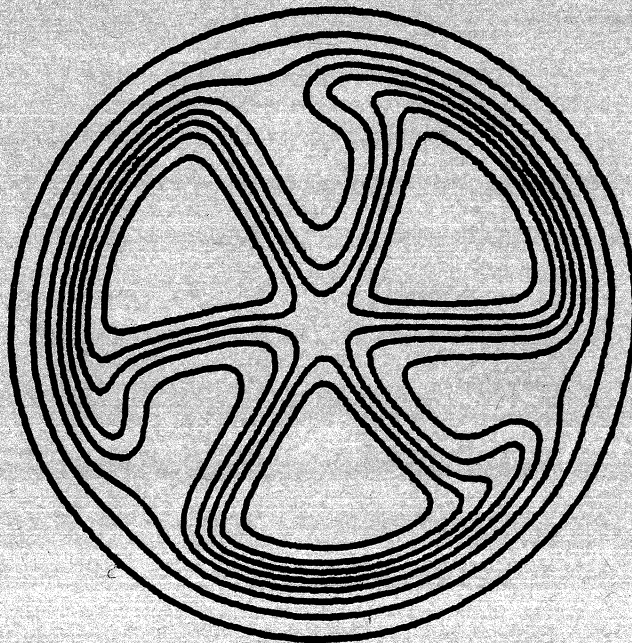
*Our files*

MICHIGAN STATE UNIVERSITY

CYCLOTRON LABORATORY

ORGANIC SCINTILLATOR PULSE SHAPE DISCRIMINATOR SIGNATURES  
ASSOCIATED WITH HIGH ENERGY NEUTRONS

R. St. ONGE, AARON GALONSKY, R.K. JOLLY, and T.M. AMOS





## I. INTRODUCTION

In traversing matter, a charged particle produces an ionized track. The specific ionization density of this track is dependent upon the energy, charge, and mass of the particle. If the material traversed is an organic scintillator, the molecular modes excited are observed to depend upon the specific ionization.<sup>1</sup> The resultant de-excitation by scintillation can usually be described as the sum of two exponential decays whose relative intensities and decay time constants are dependent upon the charged particle.<sup>2</sup> Although additional decay components may be involved, their relative contribution is usually negligible.<sup>3</sup> Thus, two charged particles of different mass or charge will produce two different scintillation light histories.<sup>4</sup> The exploitation of this dependence of the scintillation history on the specific ionization density in the track of the exciting particle is a method of discriminating amongst different particle types.<sup>5</sup> This experimental technique is commonly called pulse shape discrimination (PSD).

A number of methods of PSD have been presented in the literature. These methods vary widely in resolution, complexity, and dynamic range.<sup>6</sup> Our use of PSD was for (p,n) time-of-flight (TOF) experiments.<sup>7</sup> These experiments required excellent particle resolution between neutron and gamma-ray events, excellent time resolution for neutron energy determination by TOF computation, and wide dynamic pulse-height range for high efficiency. Because of the last requirement the zero-crossover method<sup>8,9</sup> of PSD was chosen. To study the information obtained from each event, all three parameters: pulse height (PH), pulse shape (PS),

Organic Scintillator Pulse Shape Discriminator Signatures  
Associated with High Energy Neutrons\*

R. St-Onge,<sup>†</sup> Aaron Galonsky, R.K. Jolly,<sup>††</sup> and T.M. Amos<sup>†††</sup>

Cyclotron Laboratory, Physics Department  
Michigan State University, East Lansing, Michigan 48824

### ABSTRACT

A two-dimensional system of pulse-shape discrimination (PSD) is described as applied to neutron time-of-flight experiments. When the detector is irradiated with neutrons and gamma rays from 40-MeV proton bombardment of <sup>7</sup>Li, five different PSD signatures are observed--one associated with gamma rays, four with neutrons. The origins of these groups are explained and their importance in neutron detection is discussed.

\* Supported by the National Science Foundation and the Office of Naval Research.

† Present address: University of New Hampshire, Dept. of Physics, Durham, N.H. 03824

†† Present address: College of William and Mary, VARC, Newport News, Va. 23606

††† Present address: Brown and Root, Inc., P.O. Box 3, Houston, Texas 77001

and TOF were analyzed on-line. The PSD system was used to separate neutron from gamma-ray events. This combination of high resolution PSD and TOF systems allowed identification of previously unnoticed PSD signatures.

## II. THE EXPERIMENTAL SYSTEMS

### a. The Cyclotron

The Michigan State University Isochronous Cyclotron is a variable-energy instrument capable of producing beams of protons with energies up to 50 MeV with a micro-burst time-width of less than 0.3 nanosecond (FWHM).<sup>10</sup> This feature has been vital in neutron TOF experiments because only a short flight path is available.

### b. The PSD - TOF System

The detector is an NE 213 organic scintillator sealed within a cylindrical glass cell with inside dimensions of 4.44 cm diameter by 1.91 cm deep. On one side of the cell is a standard small thermal expansion chamber. The main body of the cell is painted with several coats of Eastman White Reflectance paint while the expansion chamber is covered with flat black paint. The scintillator cell is vacuum potted with clear Dow Corning Sylgard to a selected RCA 8575 phototube. The phototube is attached to a constant-fraction base<sup>11</sup> which is cooled by a small blower to insure temperature stability. The dynode voltages are optimized for pulse-height resolution of the pair of <sup>60</sup>Co gamma-ray lines. This resolution (~7% FWHM) is sufficient to

resolve the resultant two Compton edges as shown in Fig. 1. It appears that good pulse-height resolution contributes to good PSD.

The PSD System shown in Fig. 2 fans out from a constant-fraction phototube base from which a pulse-height signal is fed to a delay-line amplifier from which two different signals are extracted; a unipolar single delay-line signal and a bipolar double delay-line signal. The first is used for pulse height (PH) analysis and the latter signal is fed into a combination single-channel analyzer and zero-crossover detector to obtain a fast logic signal.

The event-logic signal is first fed into a wide-band amplifier and then into a 1  $\mu$  sec roll of RG-8 coaxial cable. The cable-delayed logic signal is combined in a time-to-amplitude converter with the zero-crossover logic signal to obtain the pulse shape (PS) signal. Use of the cable delay, instead of a modular electronic logic delay, improved the PSD resolution by eliminating the greater output jitter and the greater thermal shifts of the module.

The TOF system, also shown in Fig. 2, measures the time difference (TOF) between the event-initiated constant-fraction time signal and a zero crossover time signal derived from the cyclotron rf picked up by a small inductor near the dees of the cyclotron.

The PSD-TOF system presents the three pulses (PH, PS, and TOF) to three analog-to-digital converters whose digital outputs are interfaced to an on-line computer.

### C. The On-line Computer

Particle intensity with the three data words form a three parameter, four dimensional data pad in the computer. "Tootsie", an on-line, time-shared, data-taking program, provides a fast, flexible method of particle identification for the Michigan State University Xerox Data Systems Computer, Sigma-7.<sup>12</sup> Data are stored in a 16K bin, two parameter (PH x PS) analyzer and displayed on a storage scope. Such a display, to be discussed later, is shown in Fig. 3. Separate regions of interest in the display can be defined by fitting polynomials to the boundaries of the data groups. For each region one parameter TOF spectrum is generated by the interrupt servicing routine using a table look-up computer mode.

### III. EXPERIMENTAL RESULTS

#### A. Pu-Be Test Data

To test the quality of the PSD system we recorded the PH x PS spectrum from a Pu-Be neutron, gamma-ray source. The data are shown in Fig. 4, an orthographic projection<sup>13</sup> which gives the intensity surface as a function of the two PSD parameters. This type of plot conveys the intensity information much more quantitatively than does the scope display, but only the latter is available in real time. Separation of neutrons and gamma rays is clearly very good.

A standardized quantitative measure of the pulse-shape resolution of the system can be obtained by considering a figure

of merit,  $M$ , defined as the separation of the peaks divided by the sum of the full widths at half maximum of the two peaks.<sup>14</sup> As seen in Fig. 4, the separation (and  $M$ ) is clearly a function of pulse height. At a pulse height indicated by the arrow in Fig. 4, namely 2.12 MeV (twice the <sup>22</sup>Na Compton edge), a 5% thick slice of data is shown in Fig. 5. At this pulse height  $M=5.2\pm 0.1$ . The  $M$  value varies from approximately 3.5 at the low PH end of Fig. 4 to 5.5 at the high PH end.

#### B. Response to Radiation from <sup>7</sup>Li + p at 40 MeV

The <sup>7</sup>Li(p,n) reaction has a large yield of neutrons to the ground and first-excited states of <sup>7</sup>Be and a tail of lower-energy neutrons from excitation of unbound states and from multi-body breakup;<sup>15</sup> it is thus a source of almost-monoenergetic neutrons. We used this source to study the response of our detector to neutrons of substantially higher energy than is emitted from a Pu-Be source. The detector was placed 3.5 m at 20° from a 25 mg/cm<sup>2</sup> <sup>7</sup>Li target bombarded with 40-MeV protons. The average energy of the ground-state neutrons was 37.5 MeV.

The resulting 2-parameter PH x PS display is that already shown in Fig. 3, its orthographic projection is presented in Fig. 6. In each of these figures there are five obvious groups, labelled A through E, although only neutrons and gamma rays could have reached the detector. Groups A and C have the same PSD signatures obtained from the Pu-Be source for gamma rays and neutrons, respectively.

To help identify the parentage of the other groups, we defined each of the five groups with polynomial boundaries and measured the TOF spectrum of each group. These spectra are shown in Fig. 7. Some of each spectrum appears twice. Doubled spectra were obtained by sending alternate, rather than consecutive, rf stop pulses to the TOF TAC. (See Fig. 2.) A doubled spectrum provides a built-in time calibration, the time between corresponding features of the spectrum being one rf period. In the present case we have 54 nsec equivalent to 409 channels.

In TOF spectrum A, the gamma-ray spectrum, gamma rays from the target peak in channel 390. Protons scattered by the target into the walls of the target chamber produced the tail which extends down to about channel 350. The peaks around channels 149 (and 558), 165 (and 574), and 212 also originated where scattered protons struck parts of the apparatus. These four sources of gamma rays have, in each case, been eliminated or greatly diminished and will not be further discussed here. The important part of the gamma-ray spectrum is the target peak, since it is used with the flight path and channels-to-time calibration to convert channel number into neutron energy.

In TOF spectrum C, where we expect neutrons, we do see the expected--a strong peak in channel 566 (and 167), just where the 37.5-MeV, ground-state neutrons should be. (A small contribution from excitation of the first-excited state of  $^7\text{Be}$  at 0.43 MeV would not be resolved from the ground-state group.) Furthermore, the peak in channel 546 (and 137) for  $E_n=33.0$  MeV correlates with

excitation of the second-excited state of  $^7\text{Be}$  at 4.55 MeV. We note that the TOFs or channel numbers, of the peaks in A and in C are mutually exclusive.

It is clear from Fig. 7 that the three additional PSD signatures -B, D, and E--specify neutrons, not gamma rays. How do these groups arise?

B arises from a finite-size effect in the scintillator, specifically, from n-p scattering so far back in the scintillator that the protons recoil out the end of the scintillator. For example, consider some 37.5-MeV recoil protons. Compared to one which stops in the scintillator, the PH from one which leaves the scintillator after losing only 5 MeV will be much lower. The latter proton will, in addition, produce a larger PS signal because  $dE/dx$  of a 37.5-32.5 MeV proton is much less than  $dE/dx$  of a stopping 37.5-MeV proton. The PS of the lightly-ionizing, escaping proton resembles that of the Compton electrons in group A more than that of the stopping protons in group C. Hence, our escaping proton makes a small PH and a large PS; in Figs. 3 and 6 it can be found just under the base of group A. Another escaping 37.5-MeV proton which deposits more than 5 MeV in the scintillator produces a larger PH and a smaller PS. The greater the energy loss, the closer the two-dimensional position to that of a stopping 37.5-MeV proton. Similar considerations apply to recoil protons of lower energies, but of course, the lower the energy, the smaller the range, and the less important this end effect. The composite effect should produce all of the group-B features seen in Figs. 3 and 6.

It is clear that the importance of the end effect increases with neutron energy. One can see this in Fig. 7 where the low-energy tail in spectrum B falls off much more rapidly than in spectrum C. The other relevant parameter is scintillator thickness -- the thicker the scintillator, the smaller the end effect. It is important in computing the neutron efficiency of a detector to know how the end effect is treated and to treat it accordingly when taking data. In one-parameter PSD, i.e. when PH is not distinguished, end-effect neutrons can appear as a tail or satellite hump on the gamma-ray peak and be erroneously excluded from the selected neutron group.

D and E arise from neutron interactions with the carbon of the scintillator. In D we have protons, mainly from  $^{12}\text{C}(n,p)^{12}\text{B}$ , and in E alpha particles, mainly from  $^{12}\text{C}(n,n^3\alpha)$ . As the Q values for these reactions are -12.6 MeV and -7.3 MeV, respectively, the maximum PHs in D and E are less than in C. In E the maximum PH is also substantially reduced because of the low light-producing efficiency of alpha particles in comparison to protons,<sup>16</sup> which are more lightly ionizing. Twenty-MeV alpha particles, for example, produce as much light in NE-213 as do 11.5-MeV protons.<sup>16</sup>

The PS signals for D and E are also lower than for C. That this should occur for E, in which alpha particles are the origin of the light, is a routine illustration of the relationship between scintillation decay time and ionization density. The shift of D from C must be attributed to the same kind of relationship, with the dense ionization produced by recoils of reaction products, mainly  $^{12}\text{B}$  ions. This is true in spite of the

fact that the light produced by  $^{12}\text{B}$  ions in the  $^{12}\text{C}(n,p)^{12}\text{B}$  reaction is negligible in determining PH. For example, with a 37.5-MeV neutron producing a 20-MeV proton at  $90^\circ$ , the  $^{12}\text{B}$  recoils with 5 MeV and makes 1% of the light<sup>16</sup> for the event.

The relative intensities of C, D, and E are consistent with the cross sections<sup>18</sup> for n-p scattering, for  $^{12}\text{C}(n,p)$ , and for  $^{12}\text{C}(n,n^3\alpha)$ .

An understanding of the fine structure in PSD, particularly of the origin of E, has been useful in TOF experiments.<sup>18</sup> Because the  $^{12}\text{C}(n,n^3\alpha)$  cross section is poorly known, E was excluded from the data and from the detection efficiency computed with Kurz's program.<sup>19</sup> At a small cost in efficiency the absolute accuracy was improved.

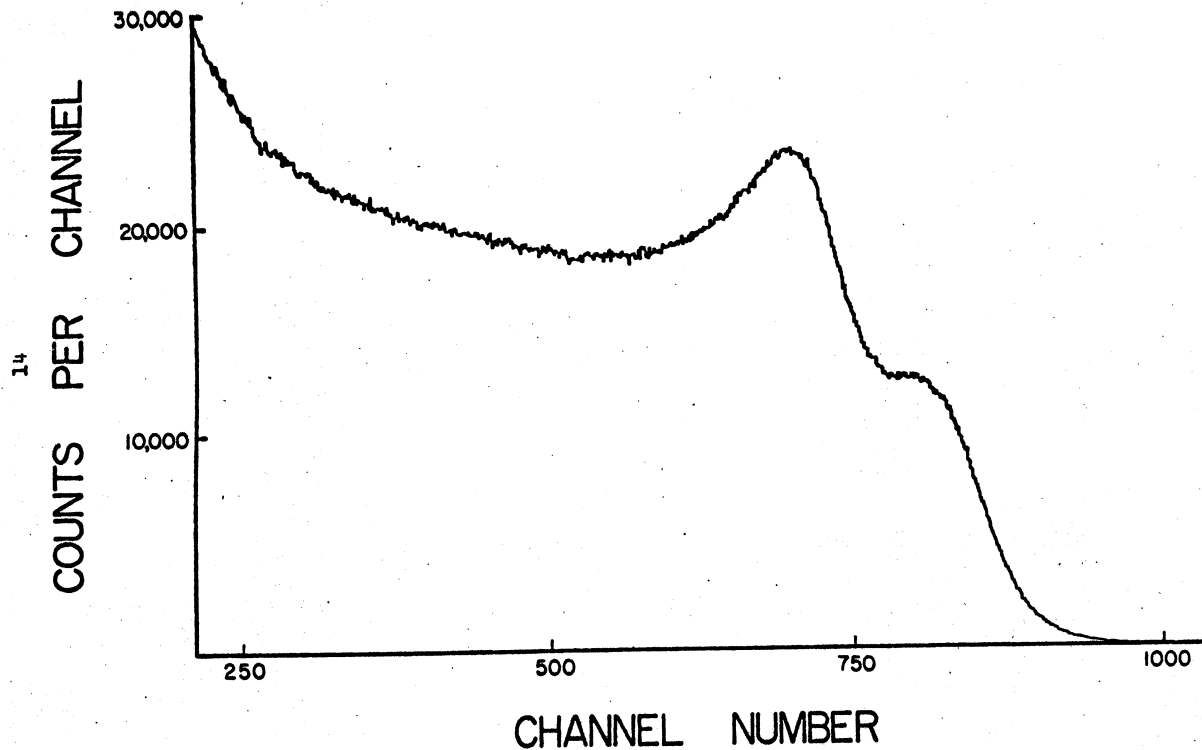
In neutron spectroscopy not involving TOF, understanding PSD fine structure should also be important. Scintillation detectors are used to measure neutron spectra in the upper atmosphere<sup>20</sup> and in the Van Allen belts. Above about 50 MeV, neutron interactions in carbon predominate over n-p scattering. Groups D and E should make a high-efficiency, excellent replacement for group C above 50 MeV. In a calibration experiment it should be possible to improve the accuracy of the carbon cross sections by careful observation of C,D,E simultaneously as a function of neutron energy.

## REFERENCES

1. R.B. Owen, I.R.E. Trans. On Nuclear Science NS-5, N.3(1958)198.
2. P.G. Sjoelin, Nucl. Instr. and Meth. 37(1964)45.
3. F.B. Harrison, Nucleonics, 12(1954)24.
4. F.T. Kuchnir and F.J. Lynch, IEEE Trans. Nucl. Sci. NS-15, No. 2(1968)10.
5. F.D. Brooks, Brit. Patent Spec. 823263(1957).
6. R.N. St. Onge and J.A. Lockwood, Nucl. Instr. and Meth. 69, (1969)25.
7. R.K. Jolly, T.M. Amos, A. Galonsky, R. Hinrichs and R. St. Onge, Phys. Rev. C7 (1973)1903.
8. T.K. Alexander and F.G. Goulding, Nucl. Instr. and Meth. 13 (1961)244.
9. G.W. McBeth, J.W. Lutkin, and R.A. Winyard, Nucl. Instr. and Meth. 93 (1971)99.
10. S.P. Johnson, H.G. Blosser, and R.N. St. Onge. Proceedings of the International Cyclotron Conference, Oxford, England, Sept., 1969.
11. Ortec, Inc. Model 270, Constant Fraction Discriminator Base.
12. D.L. Bayer, the Data Acquisition Task Tootsie, Michigan State University Cyclotron Laboratory Report - 34.
13. Computer-plotted via a computer program of D.A. Johnson, Michigan State University Cyclotron Laboratory.
14. W.B. Reid and R.H. Hummel., Can. Nucl. Tech. (Jan-Feb, 1966).
15. J.W. Wächter, R.T. Santoro, T.A. Love and W. Zobel, Nucl. Instr. and Meth. 113 (1973)1850 and J.A. Jungerman, F.P. Brady, W.J. Knox, T. Montgomery, M.R. McGie, J.L. Romero and Y. Ishizaki, Nucl. Instr. and Meth. 94 91971)421.
16. A Huck and G. Walter, Nucl. Instr. and Meth., 59 (1968)157.
17. V.V. Verbinski, W.R. Burrus, T.A. Love, W. Zobel, N.W. Hill, and R. Textor, Nucl. Instr. and Meth. 65 (1968)8.
18. R.R. Doering, D.M. Patterson and Aaron Galonsky, submitted to Physical Review.
19. R.J. Kurz, UC-34 Physics, TID-4500 (24th Ed.) Univ. of Cal., A709/7090 Fortran II Program to Compute the Neutron-Detection Efficiency of Plastic Scintillator for Neutron Energies from 1 to 300 MeV.
20. J.A. Lockwood, R. St. Onge, D. Klumpar, and D. Schow, Acta Physica Academiae Scientiarum Hungaricae 29, Suppl. 2 (1970) 703. (Proc. 11th Int. Conf. on Cosmic Rays, Budapest 1969).



# $^{60}\text{Co}$ PULSE HEIGHT SPECTRUM IN NE-213



13

## FIGURE CAPTIONS

Figure 1.--Pulse-height spectrum of  $^{60}\text{Co}$  gamma rays in the NE-213 scintillation detector.

Figure 2.--Block diagram of the electronics.

Figure 3.--Oscilloscope photograph of intensity vs. pulse height (PH) and pulse shape (PS) for events in the scintillation detector when exposed to radiation from a  $^7\text{Li}$  target bombarded by 40-MeV protons.

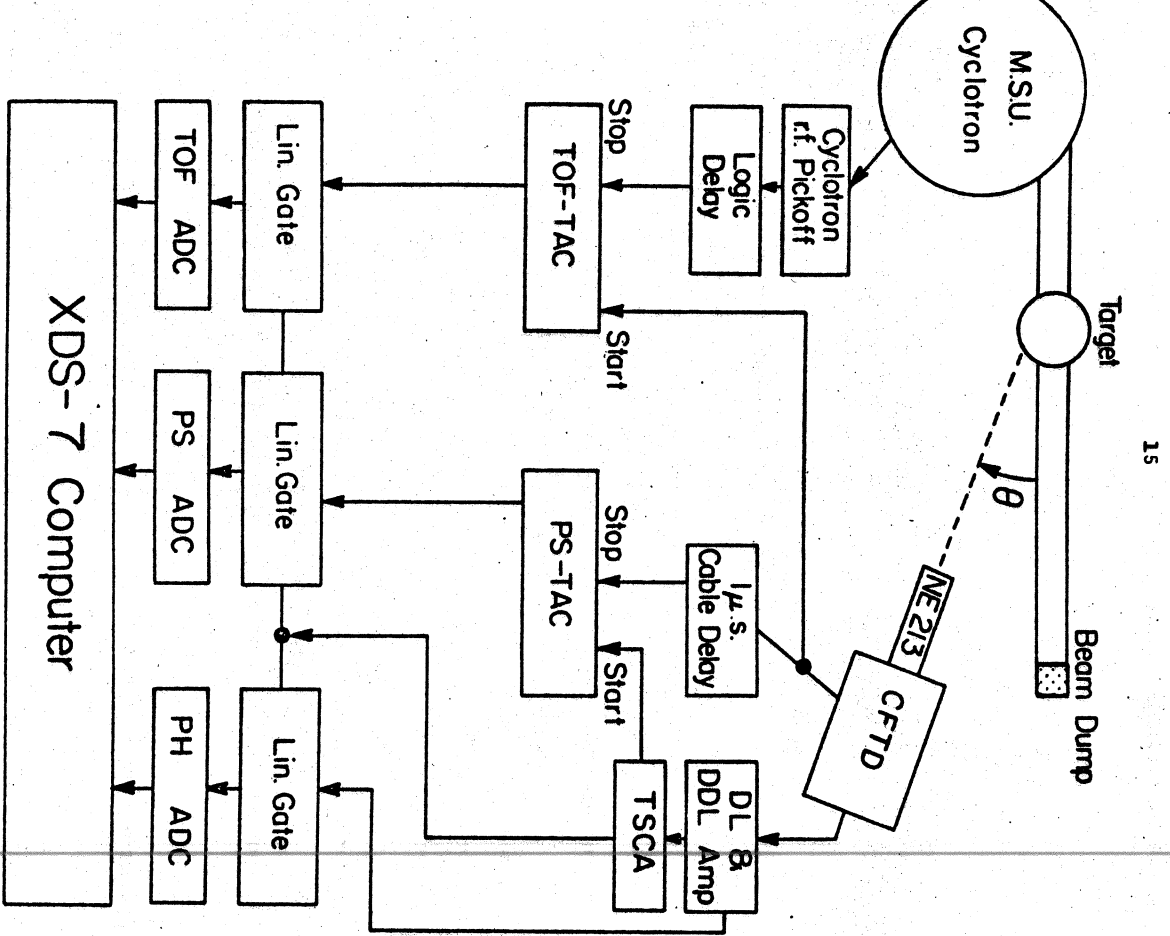
Figure 4.--Orthographic projection of intensity vs. pulse height (PH) and pulse shape (PS) for events in the scintillation detector when exposed to radiation from Pu-Be neutron, gamma-ray source. Arrow is at PH=2.12 MeV.

Figure 5.--Pulse shape discrimination spectrum of events in

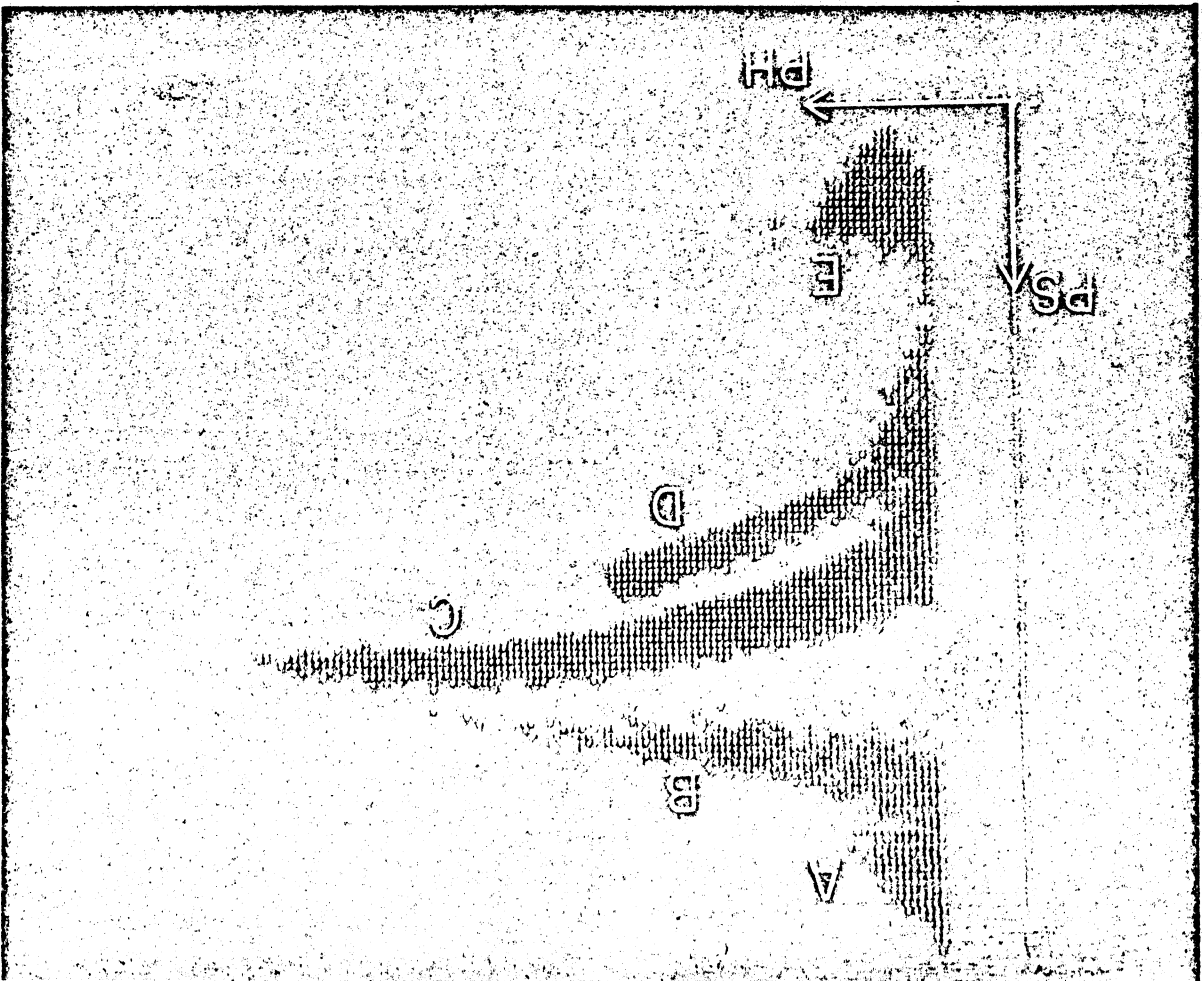
Fig. 4 having PH=2.12 MeV (see arrow in Fig. 4).

Figure 6.--Orthographic projection of data in Fig. 3.

Figure 7.--Time-of-flight spectra of the groups, A through E, in Figs. 3 and 6.

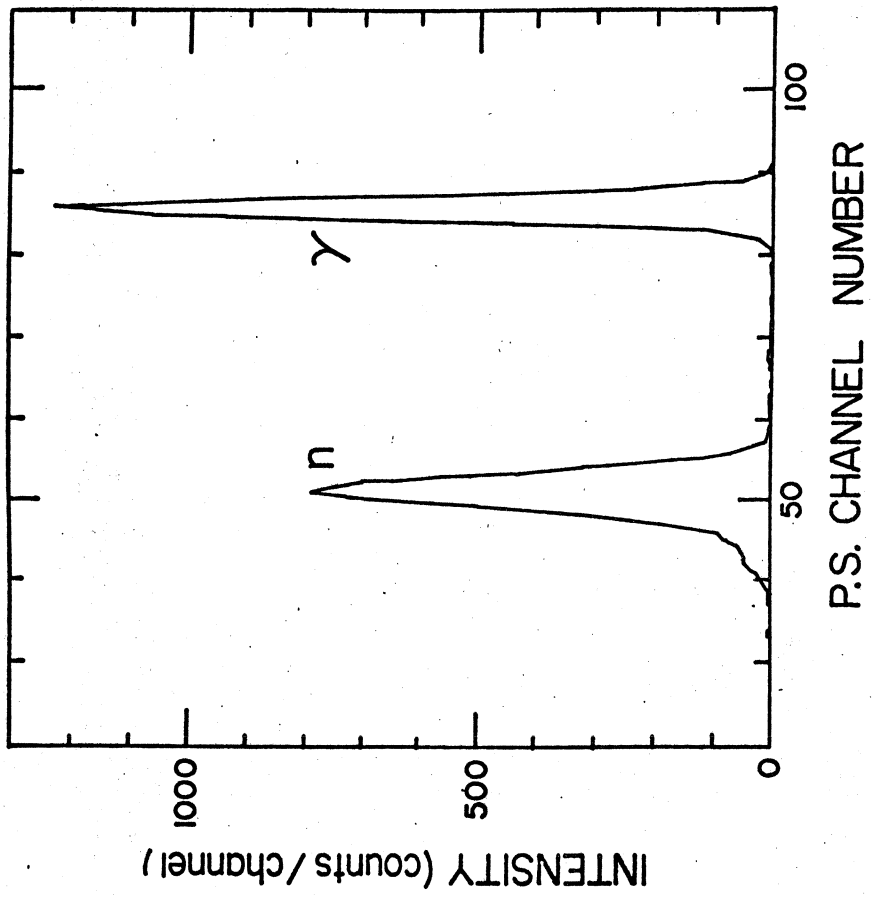


15

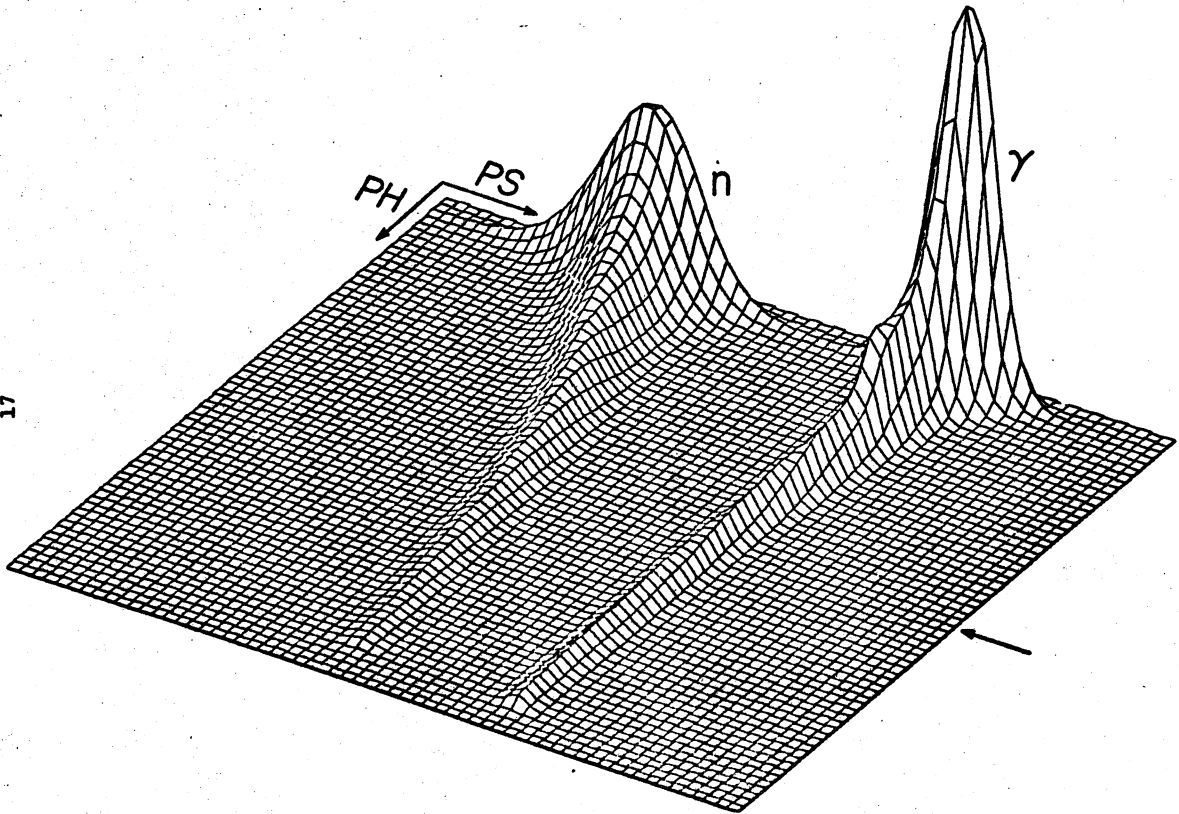


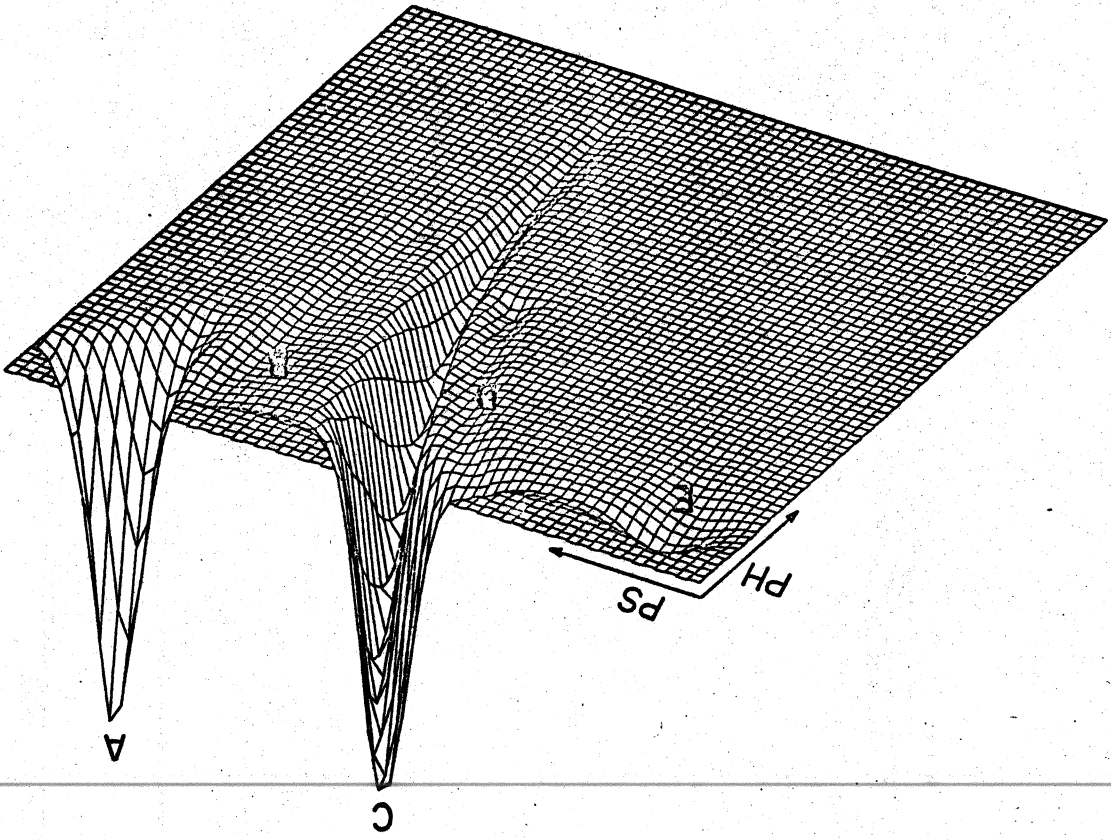
16

18

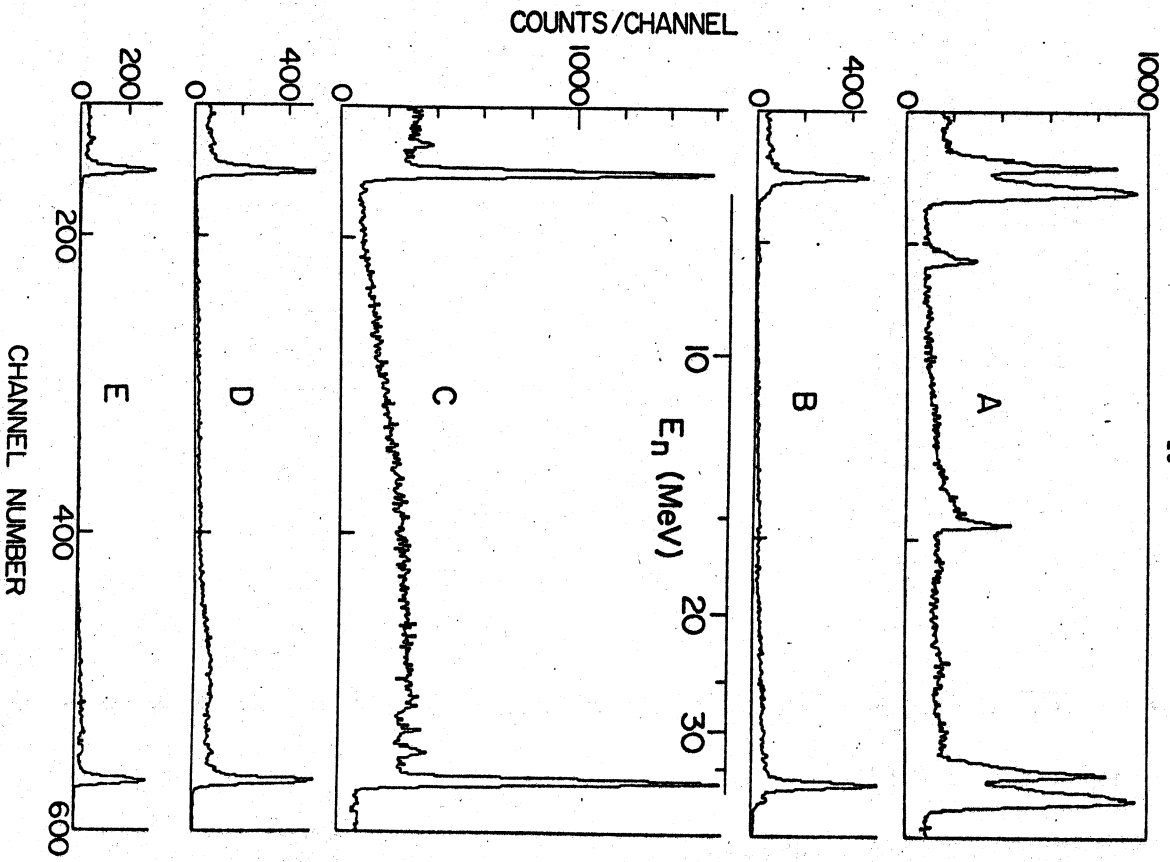


17





19



20